Radiative Widths, Spins, and Parities of Nuclear Levels in the 6–9-MeV Region Excited by Neutron Capture γ Rays

R. Moreh, S. Shlomo, and A. Wolf
Nuclear Research Centre, Negev, Beer-Sheva, Israel
(Received 23 April 1970)

Monochromatic photons obtained from thermal-neutron capture in iron were used for exciting nuclear levels in the energy region between 6 and 9 MeV. Angular distribution of the elastically scattered radiation was carried out for the determination of the spins of the resonance levels. Total and ground-state radiation widths of ten resonance levels in various isotopes were measured using self-absorption, temperature variation, and absolute scattering cross-section measurements. The parity of six resonance levels was measured using a Compton polarimeter, and strong $M1$ transitions were found in ^{141}Pr and ^{208}Pb; the character of four transitions was found to be $E1$. The observed total radiation widths Γ_γ of these bound levels were found to have the same magnitude as those of unbound levels obtained in neutron resonances, which indicate that Γ_γ is continuous across the (γ, n) threshold.

I. INTRODUCTION

The use of capture γ rays for exciting nuclear levels was started several years ago.[1-3] The most extensive work was done by Ben-David *et al.*,[3] who found about 50 resonances using different combinations of source and target. The basic idea in this technique is that a resonance event is obtained only when a random overlap exists between at least one of the incident γ lines and one level in any isotope of the target studied. This condition of random overlap places a severe limitation on the choice of the target. The present method of exciting nuclear levels has by now found a wide use in nuclear spectroscopy. The spectroscopic properties which may be measured are summarized in the following:

(1) excitation energies of the resonance level and of new low-lying levels of the scattering isotope;
(2) the spins of the resonance and of low-lying levels;
(3) the parities of the resonance levels and of low-lying levels;
(4) the total and partial radiative widths of the resonance level;
(5) statistical information regarding level spacings and level widths may be extracted from the data.

It is thus possible to study absolute values of strengths of high-energy $E1$ and $M1$ transitions; in addition, useful information regarding the amplitudes of $E2$ admixtures in $M1$ transitions may also be obtained.

In the present work, the resonance scattering of Fe capture γ rays was used to excite nuclear energy levels in several nuclei at about 7-MeV excitation. The total and partial radiative widths were measured for ten nuclei. In addition, the spins and parities of some of these levels were obtained by measuring the angular distribution and polarization of the scattered radiation.

In order to determine the ground-state radiation width Γ_0 of the resonance level, it is necessary to measure all the other parameters of the level, namely, J, δ, Γ_0/Γ_γ, where J is the spin of the level, δ is the separation energy between the peaks of the resonant line and incident line (after correcting for the recoil energy), and Γ_0/Γ_γ is the ratio between the ground-state radiation width and the total radiative width of the level. It is clear that four experiments are needed to determine these parameters. The spin J is obtained by measuring the angular distribution of the elastically scattered line. The value of Γ_0/Γ_γ may be directly obtained from the scattered radiation spectrum (after accounting for the angular distribution of the elastic and inelastic lines). The remaining two parameters δ and Γ_0 may be found by the temperature-variation experiment and a self-absorption experiment.[4-6] In the first, the ratio between the resonant scattering cross section at liquid-nitrogen temperature (80°K) and at room temperature is measured. The result of this experiment is most sensitive to the value of δ and only weakly dependent on the value of Γ_γ and Γ_0. In the second experiment the self-absorption ratio related to nuclear absorption of a resonant absorber is measured. This ratio is very sensitive to the value of Γ_0 and only weakly dependent on δ and Γ_γ. Combining the results of these two experiments, the values of δ and Γ_0 were obtained. The consistency of the parameter values was checked by using a fifth experiment in which the absolute scattering cross section of the elastically scattered radiation was measured. This cross section is very sensitive to the values of all four parameters and therefore is very suitable for this check.

For unbound levels, another unknown should be considered, namely, the neutron width Γ_n of the

resonance state. In this case, all five experiments are required to determine the five parameters. The total width $\Gamma = \Gamma_n + \Gamma_\gamma$ is obtained from absolute cross-section measurements, while the value of Γ_γ is obtained from a branching-ratio measurement. The value of Γ_n may then be determined from the difference between Γ and Γ_γ. The exact procedure for determining the level parameters will be discussed in Sec. III E.

One remark should be added regarding the sign[5] of δ. Because of the symmetric shapes of both the incident and the resonance lines, the sign of δ can not be determined by the temperature-variation experiment; it can be obtained by rotating the scatterer[7] for producing small Doppler shifts of the resonance energy. It can also be obtained by measuring the self-absorption at small angles where the energy of the scattered photons are close to the resonance energy.[8] In the remainder of this text, we shall always refer to "δ" irrespective of its actual sign.

The use of the present method for measuring the radiative widths of some resonance levels was made previously by many investigators.[5,6,9] In particular, the resonances in ^{208}Pb, ^{205}Tl, ^{112}Cd, and ^{62}Ni were reported in the literature; large discrepancies were obtained only for the level in ^{112}Cd and ^{62}Ni.

A brief mention of some of the results of the present work was made earlier.[10,11]

II. MATHEMATICAL ANALYSIS

In the following, the mathematical expressions for the experimentally measured magnitudes are given. The geometrical arrangement for the experiment is given in Fig. 1. In order to obtain the yield of the scattered radiation,[4,5] one should consider an incident γ beam whose normalized energy spectrum is given by $F_D(E)$. One may then first calculate the scattered intensity from an element of width dx from the scatterer at temperature T and account for the electronic and nuclear absorption cross section σ_e and $\sigma_n(E)$ of the incident beam. For large scattering angles, only atomic absorption of the scattered beam should be taken into account and no nuclear absorption should be assumed to occur, because at these angles the energy of the photons is smaller than that of the incident beam and therefore are removed from the resonance condition. If one denotes the elastic scattering cross section by $\sigma_r(E)$, then the elastically scattered intensity at an angle θ per unit flux of the incident beam per steradian from a scatterer (at an absolute temperature T) of infinite area may be obtained by integration over the thickness A of the scatterer and over the energy spectrum of the incident photon line. The result is given by[5]

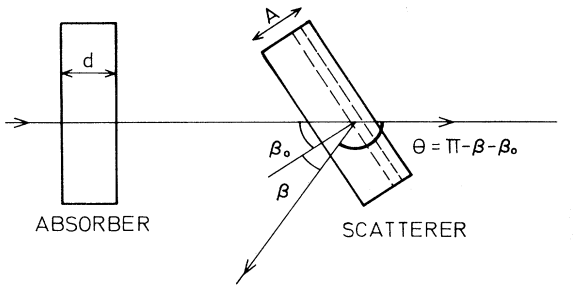

FIG. 1. Schematic description of the scatterer-absorber geometry.

$$C(T,\theta) = \int_0^\infty S(E,\theta)\,dE\,, \tag{1}$$

$$S(E,\theta) = G F_D(E)\sigma_r(E)\left[1 - e^{-NA(F_1+F_2)}\right]/(F_1+F_2)\,, \tag{2}$$

where G, F_1, F_2, and σ_r are defined by

$$G = \alpha(1+B\cos^2\theta)/4\pi(1+\tfrac{1}{3}B)\cos\beta_0\,,$$

$$F_1 = [\sigma_e + \alpha(\Gamma/\Gamma_0)\sigma_r(E)]/\cos\beta_0\,,$$

$$F_2 = \sigma_e/\cos\beta\,,$$

$$\sigma_r(E) = \Gamma_0\sigma_n(E)/\Gamma\,,$$

N is the number of target nuclei per unit volume, α the abundance of the isotope responsible for resonance scattering, and B, the coefficient of angular distribution of the scattered radiation, is given by

$$W(\theta) \propto 1 + B\cos^2\theta\,.$$

It should be noted that the above calculation is for bound and unbound levels; however, for bound levels $\Gamma = \Gamma_\gamma$.

The normalized energy spectrum $F_D(E)$ of the incident γ line is given by[5]

$$F_D(E) = \frac{1}{\Delta_e \pi^{1/2}} \exp -\frac{(E - E_r + \delta)^2}{\Delta_e^2}\,, \qquad \delta = E_r - E_e\,, \tag{3}$$

where $\Delta_e = E_e(2kT_e/M_e c^2)^{1/2}$ is the Doppler width of the incident γ line, E_e the peak energy of the incident line, E_r the peak energy of the resonance level, M_e the mass of the emitting nucleus in the γ source, T_e the effective temperature[12] of the γ source, k the Boltzmann constant, and c the velocity of light. The nuclear absorption cross section $\sigma_n(E)$ for photons of energy E by a nuclear resonance level of peak energy E_r is given by[13]

$$\sigma_n(E) = \sigma_0^m \Psi(x_r, t_r)\,, \tag{4}$$

where $\sigma_0^m = 2\pi\lambda^2 g\Gamma_0/\Gamma$, and Γ, Γ_0 were defined earli-

er. $g=(2J+1)/(2J_0+1)$ is a statistical factor; J and J_0 are the spins of the resonance and ground states, respectively, and $\lambda=2\pi\lambda$ is the wavelength of the incident photon. The function $\Psi(x_r, t_r)$ is defined by

$$\Psi(x_r, t_r)=\frac{1}{2(\pi t_r)^{1/2}}\int_{-\infty}^{+\infty}\frac{e^{-(x_r-y)^2/4t_r}}{1+y^2}\,dy, \qquad (5)$$

where

$$x_r=\frac{2(E-E_r)}{\Gamma}, \quad t_r=\left(\frac{\Delta_r}{\Gamma}\right)^2, \quad \Delta_r=E_r\left(\frac{2kT_r}{M_rc^2}\right)^{1/2},$$

Δ_r is the Doppler width of the resonance level, M_r the mass of the scattering nucleus, and T_r the effective temperature of the scatterer.

The above expression for $F_D(E)$ is accurate only for capture states formed by neutrons of zero energy and for which the level width of the final state of the compound system is zero.

In the literature,[4,6] several approximations were suggested for calculating $C(T,\theta)$ by obtaining simple analytical expressions. In the present work no attempt was done to make any approximation, and the calculations were carried out by numerical integrations using a computer. It is worthwhile, however, to mention the value of the scattered intensity from Eq. (1) for the case of a very thin scatterer where only the first-order term of the exponential is considered, giving

$$C(T,\theta)=GNA\int_0^\infty F_D(E)\sigma_r(E)dE=GNA\langle\sigma_r\rangle, \qquad (6)$$

where $\langle\sigma_r\rangle=\int_0^\infty F_D(E)\sigma_r(E)dE$ is an effective cross section for elastic resonance scattering.

It may be shown[4] that $\langle\sigma_r\rangle$ may also be expressed in the form

$$\langle\sigma_r\rangle=\sigma_0^m\frac{\Gamma_0}{\Gamma}\Psi(x_0, t_0), \qquad (7)$$

where

$$x_0=\frac{2|E_r-E_e|}{\Gamma}=\frac{2\delta}{\Gamma}, \quad t_0=\frac{\Delta_r^2+\Delta_e^2}{\Gamma^2}$$

Hence $\langle\sigma_r\rangle$ may be calculated if the four parameters Γ, Γ_0, g, δ, are known. It can be seen that the temperature-variation ratio $C(T_1,\theta)/C(T_2,\theta)$ is also a function of Γ, Γ_0, δ, and g, and may therefore be calculated from these parameters.

For the self-absorption experiment, one should calculate the scattered intensities with a resonant and a nonresonant absorber. For a resonant absorber of N atoms per cm^3 and thickness d cm, the scattered intensity N_r is given by

$$N_r=\int_0^\infty e^{-[\alpha\sigma_n(E)+\sigma_e]Nd}S(E,\theta)dE.$$

For a nonresonant absorber of N_1 atoms per cm^3 and thickness d_1 cm, the scattered intensity N_{nr} is given by

$$N_{nr}=\int_0^\infty e^{-\sigma_{e1}N_1d_1}S(E,\theta)dE.$$

The self-absorption ratio R defined by $(N_{nr}-N_r)/N_{nr}$ is therefore

$$R=\int_0^\infty S(E,\theta)[1-e^{-\alpha\sigma_n(E)Nd}]dE/\int_0^\infty S(E,\theta)dE \qquad (8)$$

only for absorbers where $Nd\sigma_e=N_1d_1\sigma_{e1}$. Simple expressions for the temperature variation and self-absorption may be obtained for special cases.[4,6]

III. EXPERIMENTAL PROCEDURE AND RESULTS

A. Experimental System

The experimental assembly (see Fig. 2) consisted of an (n,γ) source containing 10 kg of iron in the form of five separated disks placed near the reactor core along a tangential beam port. The resulting γ beam was collimated, neutron filtered, and allowed to hit various scattering targets. The flux near the iron source is about 2×10^{13} n/cm^2 sec, yielding typical γ intensities of the order of 10^8 monoenergetic photons/cm^2 sec on the target scatterer. More details regarding the assembly were published in a previous report.[14] The scattered radiation was measured using either a 5×5-in. NaI(Tl) crystal or a 30-cc Ge(Li) diode. The spectrum was recorded with a 1024-channel TMC analyzer. These detectors were placed inside a large scattering chamber of lead having inner dimensions 150×170×70 cm^3; the thickness of the walls is 15 cm.

B. Scattering Measurements

In order to measure the scattered spectra from the various targets, the 30-cc Ge(Li) crystal was placed at an angle of 135° with respect to the incident beam. This detector was covered with 8 mm of Pb shielding for filtering out the large number of low-energy photons obtained from atomic interactions of the direct γ beam with the scatterer.

A general survey of all scattering targets was made using an iron capture γ source. Table I shows a list of all resonant targets, some of which were found to scatter more than one incident line. Note that only five resonances were observed by Ben-David *et al.*[3] using an iron γ source, while here 21 resonances are found. In fact, almost every target with $Z\geq20$ may be found to yield a scattering signal, provided the running time is long enough. This is due to higher beam intensity,

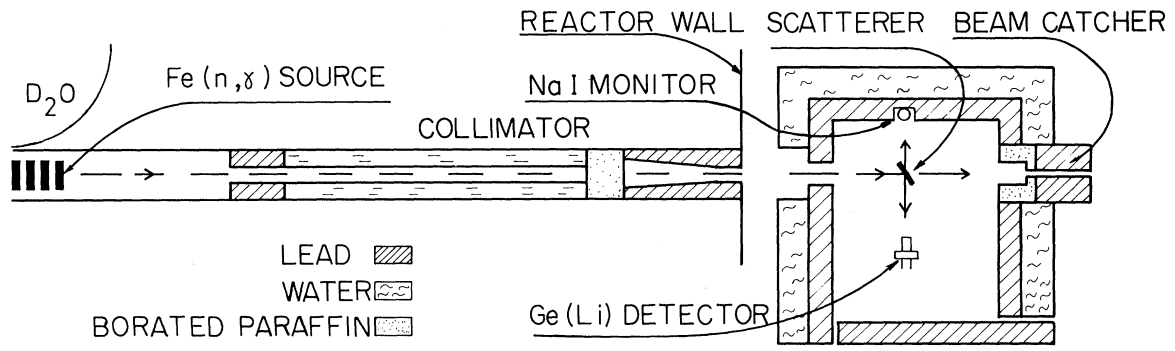

FIG. 2. Horizontal section of the experimental arrangement.

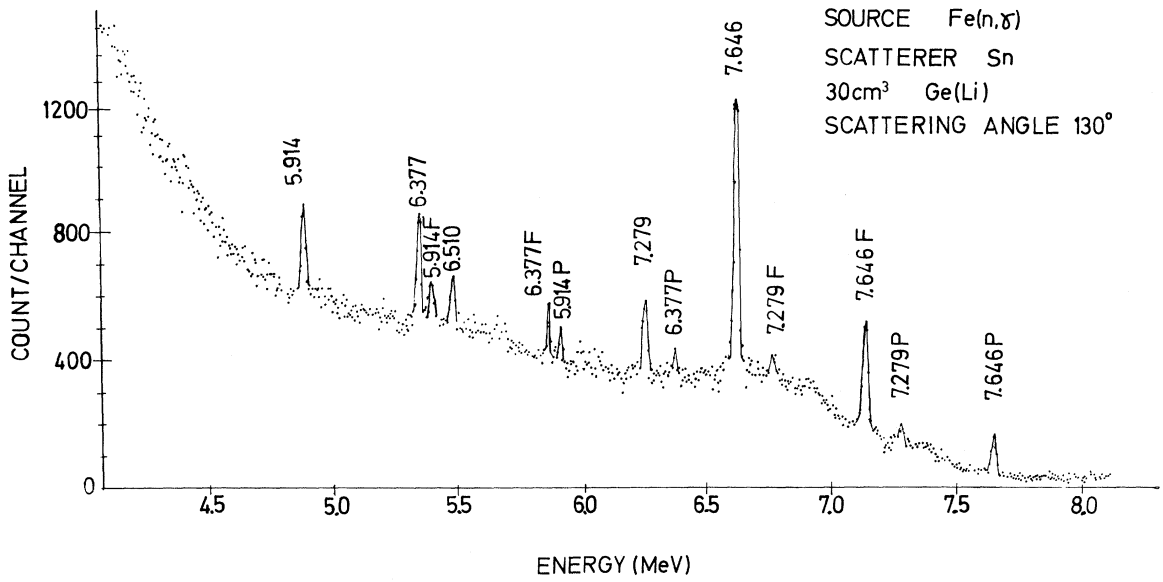

FIG. 3. Scattered γ spectrum at an angle of 130° measured by a 30-cc Ge(Li) detector. The lines at 7.646 and 7.279 MeV are independent resonances. Other lines are inelastic transitions leading to low-lying levels in one or two isotopes of Sn. Energies denoted by *P* and *F* refer to photopeaks and first-escape peaks; other energies refer to double-escape peaks.

TABLE I. List of resonant scatterers and resonant energies obtained using an Fe(n,γ) source. The isotope is specified only for cases where it was actually identified.

Strong scatterers		Weak scatterers		Very weak scatterers	
Target	Resonant energy (MeV)	Target	Resonant energy (MeV)	Target	Resonant energy (MeV)
^{62}Ni	7.646	Cr	7.646, 8.888	Mo	7.632
^{74}Ge	6.018	Zn	7.279	Nd	7.632
^{75}As	7.646	Ag	6.018, 7.632	Sm	7.632, 7.646
^{112}Cd	7.632	Sn	7.279, 7.646	Dy	7.632, 7.646
^{139}La	6.018, 7.279, 7.632	Sb	7.632, 7.646	Yb	7.632
^{141}Pr	7.632			Er	7.646
^{205}Tl	7.646			Au	7.632, 7.646
^{208}Pb	7.279			Hg	7.632, 7.646

a lower background, and the use of high-resolution Ge(Li) detectors compared with earlier work.[3] Figure 3 shows the scattered spectrum from an Sn target. This example is of interest because Sn was considered to be a nonresonant target and was used as such in the literature.[9]

C. Identification of Scattering Isotope

For some of the multi-isotopic target nuclei, it was possible to determine the isotope responsible for a resonant event by considering the energies of the inelastically scattered lines which correspond to known nuclear levels in the scattering isotope. When such evidence is not conclusive, it is possible to use a small quantity (~250 mg) of a separated isotope for identifying the scattering isotope. In such a case, the 5×5-in. NaI crystal was used for detecting the scattered radiation. This procedure was used in the case of Tl and Cr where it was found[10] that the scattering isotopes are ^{205}Tl and ^{50}Cr.

One may note that almost all observed resonance levels are bound levels. However, at least one isotope is known, namely, ^{205}Tl where the (γ,n) threshold is below the resonant energy.[10]

D. Temperature-Variation Measurement

In this measurement, the target is placed inside a Styrofoam container and the scattered intensity from the target is determined with and without liquid nitrogen inside the container; the detector used was 5×5-in. NaI crystal. Care was taken not to let any liquid nitrogen in the path of the incident beam. To get high accuracy in the present measurement, the contribution of atomic scattering and bremsstrahlung should be reduced. The normal procedure of using a "nonresonant" target for measuring this contribution at the two temperatures was found to be inadequate. This is because several of these assumed "nonresonant"-target scatterers are in effect weak resonant scatterers which may have strong temperature effects. The best procedure is to reduce the same background at the two different temperatures. This background may be easily estimated from any of the neighboring-Z "nonresonant" scatterers.

One interesting feature of the temperature effect is its relatively strong dependence on the scatterer thickness. This dependence is more pronounced for levels of large Γ_0 and is illustrated in Fig. 4 for a Pb scatterer. The temperature effect depends also on the detector angle with respect to the incident beam; this is illustrated in Fig. 5, again for a Pb scatterer. Care should be taken to account for these two factors in experimental measurements.

For calculating the effective temperature,[12] the correction curve given by Metzger[13] was used. It should be noted, however, that some large inaccuracies are expected in the determination of δ because of the strong dependence of the calculated effect on the Debye temperature Θ_D at low temperature; this is illustrated in Fig. 6. The Debye temperatures reported in the literature differ according to the particular method of measurement. A list of the values of Θ_D used in the present work is therefore given in Table II. The measured temperature effect for the various scatterers of about 10 g/cm^2 thick were found to be between 1.05 and 0.83, depending on δ and the nuclear mass of the scattering isotope.

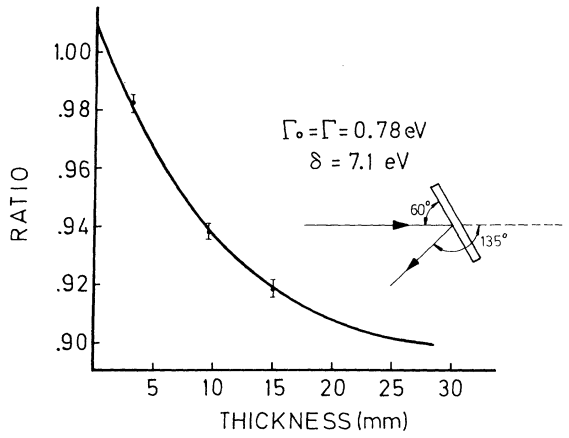

FIG. 4. Calculated and measured temperature effect (ratio of scattered signals at 80 and 300°K) for a Pb scatterer of various thicknesses. The temperature of the iron γ source is 640°K.

E. Self-Absorption Measurements

The geometry of the self-absorption measurement is illustrated in Fig. 1. In this experiment, the thickness of the two absorbers should be chosen so as to give an equal electronic absorption. The accuracy of the self-absorption measurement

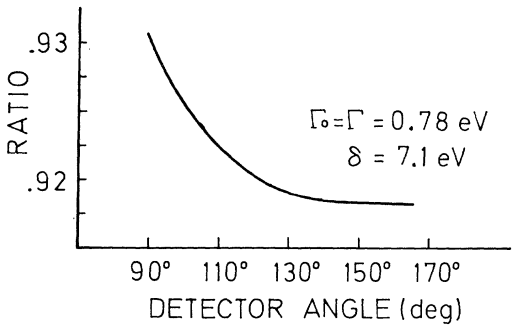

FIG. 5. Calculated temperature effect as a function of detector angle for a Pb scatterer (15 mm thick); the angle of the scatterer is 60° (see Fig. 4).

TABLE II. Debye temperature Θ_D, used for the calculation of the temperature effect and the parameters of resonance levels appearing in the present work.

Element	Θ_D (°K)
Fe	450
Cr	460
Ni	440
Ge	370
As	275
Ag	220
Cd	190
La	150
Pr	150
Tl	95
Pb	95

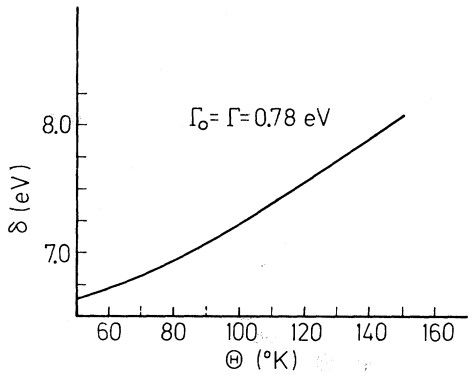

FIG. 6. The dependence of the deduced value of δ on the Debye temperature Θ_D for the case of a Pb scatterer.

is highly dependent on the accuracy of the electronic thickness of the two absorbers. In addition, since small irregularities in the density within the whole effective volume of the absorbers can introduce relatively large inaccuracies in the determination of the self-absorption ratio, an experimental check of the equivalence of the thickness of the absorbers was necessary. This check was carried out by using a γ line whose energy is near the resonance line and for which both absorbers are nonresonant. This may be illustrated for the case of Cd and In, of which Cd is resonant (7.632-MeV line) while In is nonresonant. In order to check the electronic thickness of the corresponding absorbers, a Tl target which strongly scatters the 7.646-MeV line was used, and the scattered intensities for the Cd and In absorbers were compared. Similarly, for measuring the self-absorption of a Tl absorber, the equivalent thickness of a nonresonant Bi absorber was checked by using a Cd scatterer. In fact, this method may be extended and applied for making precise measurements of attenuation coefficients of γ rays in various elements.[15] An alternative method is obtained by placing each of the two absorbers in the path of the scattered radiation in front of the NaI detector and comparing the measured intensities for the two absorbers. At large scattering angles the photons are removed from the resonance condition, and hence no nuclear absorption can take place in the resonance absorber. In order to determine the value of the parameters Γ_0 and δ from the various experiments, the following procedure[5] was adopted. The ratio of scattered intensities for two target temperatures 80 and 300°K was computed for assumed pairs of values (Γ_0, δ) such that the calculated result was equal to the experimental value. The value of J and Γ_0/Γ for this calculation was taken from experiment. In this manner, a line in the (Γ_0, δ) plane was obtained. In a similar way, another line in the (Γ_0, δ) plane was obtained by calculating the self-absorption ratio for pairs of values (Γ_0, δ) such that the result was equal to the experimental value. The point of intersection of these two lines fixed the values of Γ_0 and δ. Using these values of Γ_0, Γ_0/Γ, and δ, the value of $C(T, \theta)$ was calculated using

TABLE III. Summary of the results of spins, parities, and total widths of resonance levels excited by γ rays obtained from neutron capture in iron. Parities in parantheses are uncertain.

Isotope	Energy (MeV)	$\delta = \lvert E_r - E_e \rvert$ (eV)	J^π_0	J^π_r	Transition	Γ_0/Γ_γ (±8%)	Γ_γ (10^{-3} eV)
^{50}Cr	8.888	18 ±1	0^+	1	···	0.90	750±200
^{62}Ni	7.646	14 ±1	0^+	1^-	$E1$	0.64	480± 50
^{74}Ge	6.018	4.5±0.5	0^+	1^-	$E1$	0.19	120± 15
^{75}As	7.646	7.4±0.3	$3/2^-$	$1/2^{(+)}$	···	0.11	360±100
^{109}Ag	7.632	9 ±1	$1/2^-$	3/2	···	0.7	2± 1
^{112}Cd	7.632	4.8±0.4	0^+	1^-	$E1$	0.55	86± 15
^{139}La	6.018	8.2±0.6	$7/2^+$	$7/2^-$	$E1$	0.50	51^{+14}_{-6}
^{141}Pr	7.632	$11.4^{+0.3}_{-0.3}$	$5/2^+$	$5/2^+$	$M1$	0.46	72^{+24}_{-6}
^{205}Tl	7.646	9.3±0.3	$1/2^+$	$1/2^{(-)}$	···	0.58	980± 90
^{208}Pb	7.279	7.1±0.3	0^+	1^+	$M1$	1.00	780± 60

Eq. (1) and compared with the measured value (see Sec. III G) for checking the over-all consistency of all parameters. In some cases, large discrepancies were obtained between the calculated and measured values of $C(T,\theta)$. In the case of ^{141}Pr, the value of Γ_γ obtained without the consistency check ($\Gamma_\gamma = 0.133 \pm 0.023$ eV)[14] is much larger than the present value ($\Gamma_\gamma = 0.072^{+0.024}_{-0.006}$ eV). This may be caused by a large error in the self-absorption measurement, introduced by a weak resonance present in the "nonresonant" absorber. In such a case the values of Γ_0, Γ_0/Γ, and δ were varied within the limits of experimental errors so as to get agreement between the calculated and measured values of $C(T,\theta)$. Table III summarizes the results of Γ_0 and δ obtained from the various scatterers.

F. Angular Distributions

Angular-distribution measurements were carried out by using either a 30-cc Ge(Li) diode or a 5×5-in. NaI crystal. These detectors were mounted on an arm pivoted around a perpendicular axis passing through the scatterer. The design of the system permitted the variation of the distance between the detector and scatterer. Great care was taken to assure that the center of the collimated beam coincided with the center of the target. This was done by photographing the profile of the beam by mounting a Polaroid camera in the position of the target. The exposure time may be reduced by backing the film by a sheet of lead, which backscatters soft radiation to the Polaroid film. In an elastic resonance-fluorescence process, one deals with a cascade of the form $J_0 \to J \to J_0$, while in an inelastic process, the cascade is of the form $J_0 \to J \to J_i$, where J_0, J, and J_i are the spins of the ground, resonance, and low-lying levels, respectively. Since our main concern in the present work is with elastic transitions, the discussion is restricted in the following to this case only.

For a (γ,γ) reaction in which the transitions are of mixed dipole-quadrupole character, the angular distribution can be written as

$$W_0(\theta) = A_0^2 + A_2^2 P_2(\cos\theta) + A_4^2 P_4(\cos\theta), \qquad (9)$$

where $A_0 = 1 + x^2$, $A_2 = a + 2bx + cx^2$, $A_4 = fx^2$. The functions $P_2(\cos\theta)$ and $P_4(\cos\theta)$ are the Legendre polynomials, x is the amplitude of the mixing ratio, and a, b, c, and f are the corresponding F coefficients[16] which depend on the spin of the ground and resonance state and on the multipolarity of the transition. For pure dipole transitions, the distribution of an elastic transition takes the form

$$W_0(\theta) = 1 + a^2 P_2(\cos\theta). \qquad (10)$$

In order to find the spin of a resonance level for an assumed pure dipole transition, the experimental angular distribution should be fitted with an angular distribution of the form given by Eq. (10). The constant a^2 may be found by a least-squares fit, and the spin J of the resonance level may be deduced. By comparing the measured angular distributions of all elastic transitions with theoretical distributions, it was found that all transitions are predominantly dipole and the amplitude of quadrupole admixture was negligible. This was confirmed for most cases by the results of polarization measurement of the elastically scattered radiation. Figure 7 shows a typical angular distribution for the elastic scattering from the 7.632-MeV level in ^{109}Ag. Table III summarizes the results of spins of resonance levels.

For a mixed transition the determination of the level spin is not always unambiguous, because of the additional parameter x. Another independent experiment such as a polarization measurement of the scattered radiation is necessary in order to determine the particular values of J and x.

G. Absolute Cross-Section Measurements

The use of a Ge(Li) detector for absolute scattering cross-section measurement in the present work made it possible to obtain accuracies of the order of 6%. This is to be compared with accuracies of the order of 25% obtained when NaI detectors were used.[3,5] The intensity of the direct γ beam was measured by placing the Ge(Li) detector at the target position. To avoid pileups in this measurement, the intensity of the γ beam was reduced by using bismuth absorbers whose attenuation was determined accurately by a separate experiment.[15] Care was taken to place the entire

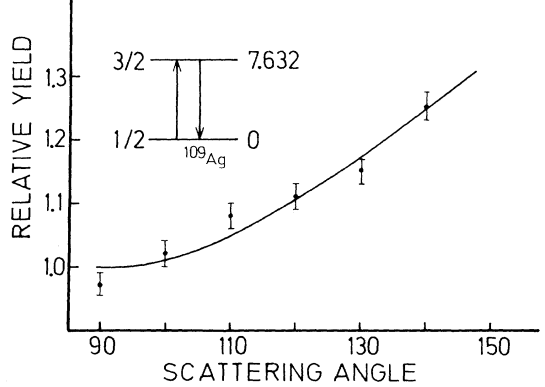

FIG. 7. Angular distribution of the elastic line in ^{109}Ag as measured using a 5×5-in. NaI detector. The solid curve shows a theoretical dipole distribution for a $\frac{3}{2}$ spin value of the resonance state.

active area of the detector in the homogenous part of the incident beam. The number of counts under the second-escape peak was taken as a measure of the line intensity; it is given by

$$N = I_i \eta_i S A_i , \tag{11}$$

where I_i is the intensity of line i in the incident γ beam, η_i the detector efficiency for the same energy line and for a collimated beam parallel to the detector axis, S the active area of the detector perpendicular to the beam direction, and A_i the total attenuation coefficient of the bismuth absorbers for the same line energy. The scattered intensity was then measured by using a thin target having a small surface area, so that the entire surface was in the homogeneous part of the incident beam. The distance r between the center of the target to the center of the detector was relatively large (about 60 cm) so that a similar beam-detector geometry was achieved for the direct-beam and scattered-beam measurements.

The number of counts under the second-escape peak of the elastically scattered line is given by

$$N_s = \frac{I_i \eta_i S S_0 C(T,\theta)\cos\beta_0}{r^2} , \tag{12}$$

where S_0 is the target area, and β_0 and $C(T,\theta)$ were defined in Sec. II. The ratio between the scattered and incident beam intensities is

$$\frac{N_s}{N_i} = \frac{S_0 C(T,\theta)\cos\beta_0}{r^2 A_i} . \tag{13}$$

Since $C(T,\theta)$ can be calculated when Γ_0, Γ_0/Γ, and δ are known and since the quantities appearing in Eq. (13) can be measured, it was possible to compare the calculated value of $C(T,\theta)$ with experiment and to check the consistency of the values of all measured parameters, as explained in Sec. III E.

Table IV gives the effective elastic scattering cross section $\langle\sigma_r\rangle$ as calculated from Eq. (6) by using the experimental values of Γ_0, Γ_0/Γ, and δ.

H. Polarization Measurements

The direction-polarization correlation of a γ-γ cascade is treated in the survey work of Biedenharn and Rose[17] and in the review article of Fagg and Hanna.[18] Here we restrict our attention again to elastic resonance scattering, i.e., to the (γ,γ) reaction only. For the case in which the transition is of mixed dipole-quadrupole character, the γ-γ direction-polarization correlation for an $M1$-$E2$ mixture is given by

$$W(\theta,\varphi) = W_0(\theta) + \cos 2\varphi\left[\left(-\tfrac{1}{2}A_2{}^2 + \tfrac{4}{3}b\,A_2 x\right)P_2^{(2)}(\cos\theta) - \tfrac{1}{12}A_4{}^2 P_4^{(2)}(\cos\theta)\right], \tag{14}$$

in which φ is the angle between the polarization vector and the normal to the resonance scattering plane, $P_2^{(2)}(\cos\theta)$ and $P_4^{(2)}(\cos\theta)$ are the associated Legendre polynomials, and b was defined in Eq. (9).

In the present work, the scattered photons were observed only at $\theta = 90°$ with respect to the incident beam. The theoretical polarization P is defined as the ratio of the linear polarization intensities parallel and perpendicular to the scattering plane. For an $M1$-$E2$ mixture, P is given by

$$P = \frac{J_{\parallel}}{J_{\perp}} = \frac{W(90,90)}{W(90,0)} = \frac{A_0{}^2 + A_2{}^2 + A_4{}^2 - 4xbA_2}{A_0{}^2 - 2A_2{}^2 - \tfrac{1}{4}A_4{}^2 + 4xbA_2} . \tag{15}$$

The polarization for pure $E2$ may be obtained from Eq. (15) by putting $x = \infty$, and for pure $M1$ by putting $A_4 = x = 0$. For an $E1$-$M2$ mixture, the polarization P is given by the reciprocal of the corresponding expression for $E2$-$M1$.

Thus for the cascade $0 \to 1 \to 0$, the polarization P is zero for $E1$ transitions and $P = \infty$ for $M1$ transitions. This means that the electric vector of the scattered radiation is completely perpendicular to the scattering plane for $E1$ transitions. This is the analog of the polarization of light in a scattering process known from classical physics.

In order to measure P, a polarization-sensitive mechanism such as Compton scattering should be employed. For plane-polarized incoming radiation,

TABLE IV. Effective elastic scattering cross section $\langle\sigma_r\rangle = \sigma_0^m(\Gamma_0/\Gamma_\gamma)\Psi(x_0,t_0)$, where δ, J, Γ_0, Γ_γ were taken from Table III. The temperature of the scatterer was 300°K, while that of the iron γ source was 640°K.

Target	Resonance energy (MeV)	$\langle\sigma_r\rangle$ (mb)
^{50}Cr	8.888	905
^{62}Ni	7.646	569
^{74}Ge	6.018	61
^{75}As	7.646	4.4
^{109}Ag	7.632	3.5
^{112}Cd	7.632	198
^{139}La	6.018	39
^{141}Pr	7.632	20
^{205}Tl	7.646	574
^{208}Pb	7.279	5560

the differential cross section for Compton scattering is given by Klein-Nishina:

$$\frac{d\sigma}{d\Omega}=\frac{r_0^2k^2}{2k_0^2}\left(\frac{k}{k_0}+\frac{k_0}{k}-2\sin^2\eta\cos^2\phi\right), \tag{16}$$

where $\phi=\varphi-90$, and k_0, k are the energies of the incident and scattered photons, respectively, the scattering angle ϕ is the angle between the plane of polarization of the incident photon and the scattering plane, and $r_0=e^2/mc^2$ is the classical radius of the electron. The energies k and k_0 are related by

$$k=k_0/[1+(k_0/mc^2)(1-\cos\eta)]. \tag{17}$$

The asymmetry ratio R is defined by $R=d\sigma(\phi=90)/d\sigma(\phi=0)$; it is a measure of the analyzing efficiency. For a given incident energy k_0, the ratio R depends on the Compton scattering angle and reaches a maximum value at a certain angle. For $k_0=7$ MeV, R reaches its maximum value at about $\eta=50°$. The degree of polarization was measured by a Compton polarimeter[19] in which the ratio $N_\parallel/N_\perp$ is determined. $N_\parallel$ is the number of γ rays Compton scattered in the plane of resonance scattering, and $N_\perp$ the number of γ rays Compton scattered in the perpendicular plane. This ratio $N_\parallel/N_\perp$ is related[19] to the theoretical polarization P by

$$\frac{N_\parallel}{N_\perp}=\frac{P+R}{PR+1}. \tag{18}$$

The values of P and R were calculated from the above equations and were corrected for finite geometry and for the detector efficiency of the scattered photons. By comparing calculated and measured values of the ratio $N_\parallel/N_\perp$, the nature of the radiation was determined.

The polarimeter[20] (Fig. 8) consists of a 1.5×2-in. NaI crystal A placed with the front face 30 cm away from the target, which served as the Comp-

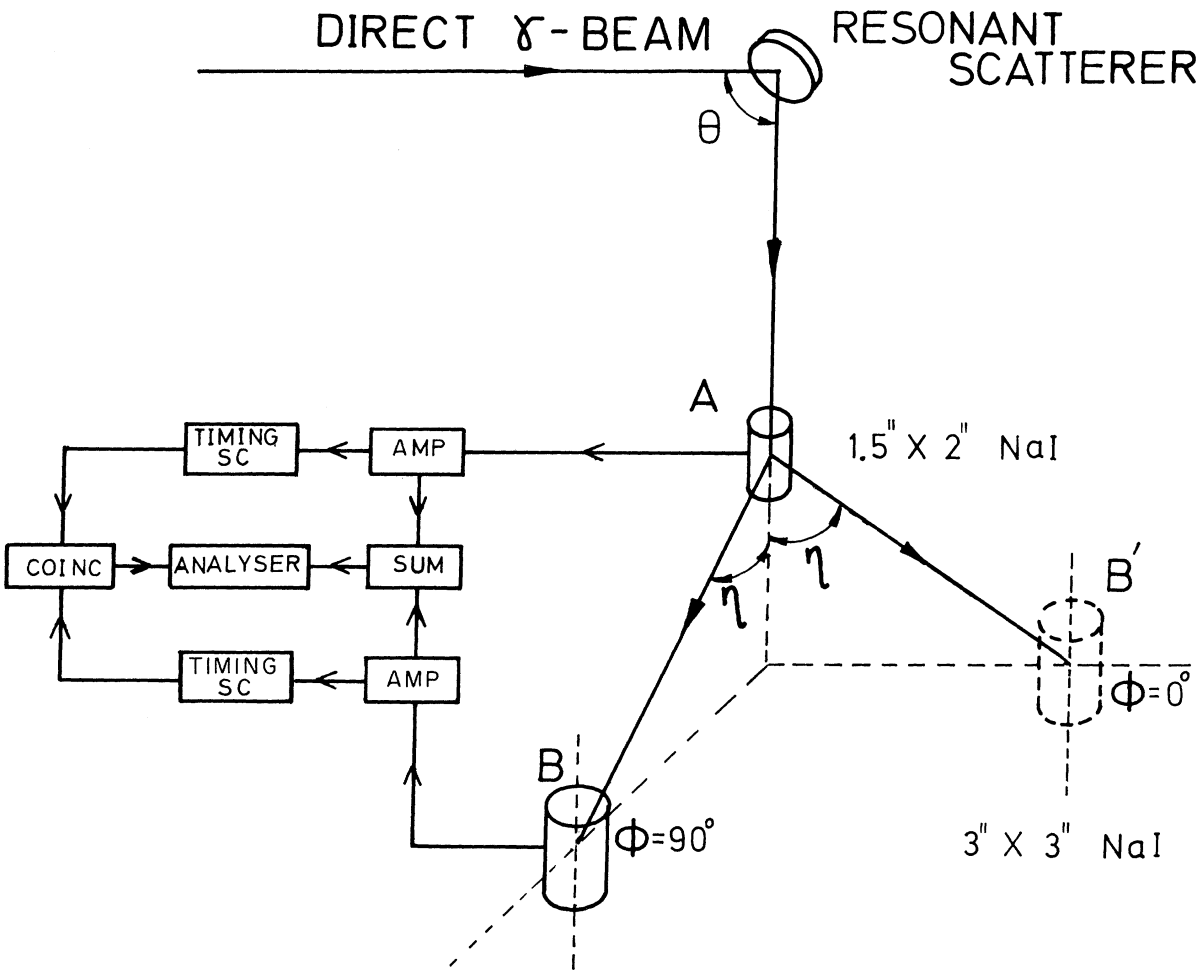

FIG. 8. Schematic diagram of the polarimeter showing also a block diagram of the electronics used in the measurement.

ton scatterer. The scattered quantum was detected in a 3×3 in. NaI crystal B which could be set in positions parallel and perpendicular to the scattering plane. The distance between the center lines of detectors A and B was 9 cm. The axis of crystal A made an angle of 90° with the direct γ beam. Absorbers of lead, iron, and paraffin were placed in front of A for filtering out the intense 0.5-MeV Compton-scattered component and the 0.511-MeV component obtained from positron annihilation in the target. For reducing background, the detectors were inserted in holes made in a large lead block (not shown in Fig. 8). The internal geometry of the block allowed the resonantly scattered-radiation to pass from the target to crystal A but not to B; it also permitted the Compton-scattered radiation to pass from crystal A to crystal B. The entire polarimeter was shielded against neutron background using 1 in. of paraffin with an inner mantel of borated plastic.

Experimentally, rather large spreads in η, θ, and ϕ were taken in order to obtain large counting rates. The spreads in these angles were $\Delta\eta = \pm 20°$ centered around $\eta = 50°$, $\Delta\theta = \pm 4°$ centered around $\theta = 90°$, and $\Delta\phi = \pm 25°$ centered around $\phi = 0$ and $\phi = 90°$. The correction due to the spread in θ is very small (~0.5%) and may be neglected; however, the spreads due to η and ϕ introduce a relatively large effect. Correcting the above spreads, the calculated ratio $N_{\parallel}/N_{\perp}$ for perfectly polarized $E1$ radiation of 7.5-MeV energy is equal to 1.15, as compared with the value 1.24 for ideal geometry. For checking the instrumental asymmetry of the polarimeter, a thallium target was used. The spin of the 7.646-MeV level in ^{205}Ti is $\frac{1}{2}$, and therefore the scattered radiation is not polarized. The ratio $N_{\parallel}/N_{\perp}$ was measured for a Tl target and was found to be 1.001 in agreement with the above expectation.

The electronics shown schematically in Fig. 8 included a fast-coincidence circuit ($2\tau = 60$ nsec) connected between detectors A and B, and a summing circuit to add coincident-pulse amplitudes provided by the outputs of the amplifiers. Single channels associated with the two detectors were used to pass all pulses falling inside the energy range of interest for the polarization measurement.

The spectrum corresponding to the other plane of the detectors was displayed on the other half of the memory of the analyzer. Figure 9 shows a typical sum coincidence spectrum at $\phi = 90$ and $\phi = 0°$ obtained using a Cd scatterer, it may be seen that the number of counts at $\phi = 0°$ is higher than that for $\phi = 90°$, which is indicative of $E1$ elastic scattered radiation. This spectrum may in principle be used to determine the parities of the low-lying excited states; however, higher statistics is generally needed for this determination.

In the actual experiment, two 3×3-in. NaI crystals were used for doubling the number of coincidence counts. Both crystals were set in the same plane with that of crystal A and were both rotated around the axis of A to go from one plane to the other. It should be noted that this polarimeter is in effect similar to that used by Bartholomew, Gunye, and Earle[21] for parity determination of levels populated through the (n,γ) reaction. However, whereas in the (n,γ) case it is necessary to perform a triple-coincidence measurement to determine the polarization, only a double-coincidence measurement is necessary in the (γ,γ') reaction because the direction of the incident beam is well defined.

Table III summarizes the results of polarization measurements and hence the parities of resonance levels. For weak resonances, (e.g., in the case of ^{50}Cr and ^{109}Ag) it was not practical to carry out the parity measurement because of the relatively high background and the inherently long running times required in such experiment.

IV. DISCUSSION

A. Γ_γ of Bound Levels

Since the excitation energies of the levels involved in the present work are in the range 6 to 9 MeV and are roughly at about the same excitation as that obtained in neutron resonances, one should

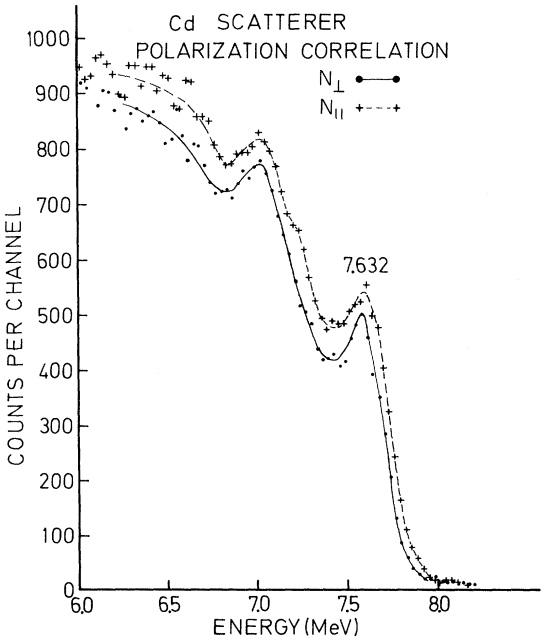

FIG. 9. Sum-coincidence spectrum as obtained with the 3×3-in. detector in planes perpendicular (⊥) and parallel (||) to the resonance scattering plane.

expect the partial and total radiative widths to obey the same statistical distributions as those of neutron resonances. In fact, almost all levels populated here are bound levels, whereas those obtained from neutron resonances are unbound levels; hence, the present work is in a sense complementary to that of neutron resonances. By comparing the radiative widths of bound and unbound levels, it will be possible to study the behavior of radiative widths across the (γ, n) threshold.

A vast amount of information was accumulated during the last ten years regarding radiative widths of neutron resonances.[22,23] The statistical distributions of partial radiative widths and total radiative widths were investigated in detail, and the systematics of the Γ_γ as a function of nuclear mass number A was also measured. The starting point of the analysis of the present data should therefore be the familiar Porter-Thomas analysis[24] of partial and total radiative widths known from neutron resonances. It is now clear that the distribution of partial radiative widths Γ_i from different initial states to the same final state is governed by a Porter-Thomas distribution, namely, a χ^2 distribution with one degree of freedom; it has the form

$$\rho(z) = z^{-1/2} e^{-z/2} ,$$

where $z = \Gamma_i/\overline{\Gamma}_i$, and $\overline{\Gamma}_i$ is the average partial radiative width. This is a very broad distribution whose 90% confidence limit includes a range of variation of more than 2 orders of magnitude. However, the distribution of the total radiative widths that proceed through ν exit channels should be a χ^2 distribution with ν degrees of freedom, i.e., a distribution of the form

$$\rho(z) = \Gamma(z/2)^{(\nu-2)/2} e^{-\nu z/2} ,$$

where $\Gamma(z/2)$ is the usual Γ function. For $\nu = 30$, this distribution is narrow; its 90% confidence limit lies between $0.7\overline{\Gamma}_\gamma$ and $1.4\overline{\Gamma}_\gamma$. Now, by considering the results of Table III, it may be seen that total radiative widths Γ_γ of the γ resonances are surprisingly close (except for ^{74}Ge) to the values of $\overline{\Gamma}_\gamma$ obtained by neutron resonances for the same or neighboring nuclei.[23] This result is at variance with that of Ramchandran and McIntyre[5] and Reibel and Mann,[25] who concluded that the Γ_γ of bound levels are about a factor of 10 larger than that of neutron resonances. This also indicates that the value of $\overline{\Gamma}_\gamma$ is continuous across the (γ, n) threshold. It may be noted that in each isotope mentioned in Table III, the Γ_γ of only one level is presented, and therefore some deviation from $\overline{\Gamma}_\gamma$ is expected within the 90% confidence limit mentioned above. Besides, another deviation is expected because of the difference in excitation energies of the resonance levels measured here and those obtained by neutron resonances. An extreme case is ^{74}Ge, where the energy of the γ-resonance level is 6.018 MeV as compared with 10.20 MeV which is the (γ, n) threshold energy. Therefore the discrepancy between the measured value ($\Gamma_\gamma = 120$ meV) for ^{74}Ge as found in the present work and the average of Γ_γ obtained from neutron resonances ($\overline{\Gamma}_\gamma \sim 300$ meV) for nuclei in the range $70 < A < 80$ is not unexpected and may be attributed to the above two factors.

B. Spacing of Bound Levels

We consider the strength function defined by $\overline{\Gamma}_\gamma/D$, where D is the spacing of levels of the same spin and parity. Assuming that this function is continuous across the (γ, n) threshold,[26] it follows from the continuity of $\overline{\Gamma}_\gamma$ that D is also continuous. The above assumption may be justified by noting that the average photon absorption cross section $\langle\sigma_n\rangle$, which is proportional[26] to $\overline{\Gamma}_0/D$ was found to be continuous across the (γ, n) threshold for a Bi target.[27] Since $\overline{\Gamma}_0/\overline{\Gamma}_\gamma$ is expected to be continuous, it follows that $\overline{\Gamma}_\gamma/D$ is also continuous across the (γ, n) threshold.

In fact, it may be shown[28] that the present measurements yield spacing values which are of about the same magnitude as those obtained from neutron resonances. One such example is ^{139}La, where the average value of the spacing of γ resonances, as obtained from the (γ, γ') reaction using several γ sources,[28] was found to be 130 eV at an excitation of about 7.5 MeV. The spacing in this context is taken between levels having one of the spin values $\frac{5}{2}$, $\frac{7}{2}$, and $\frac{9}{2}$ of both parities in ^{139}La; the ground state of this nucleus is $\frac{7}{2}^+$. This value of the spacing should be compared with a value of 100 ± 30 eV at 7.5 MeV as deduced from the observed spacing[29] of neutron resonances [23 ± 7 eV, at 8.78 MeV in the ^{138}La$(n, \gamma)^{139}$La reaction] after accounting for the difference in excitation energies and for the fact that levels with three different spins of both parities may be excited in a (γ, γ') reaction. This result is considered to be a very good agreement in view of all approximations and uncertainties involved.

The spacing of γ resonances mentioned above was obtained from experiment by making a simple statistical argument[28] and by assuming that a resonance scattering signal is detected when the incident energy is as close as 15 eV from either side of the resonance level (after recoil corrections). Another assumption was that only strong intensity lines in a γ source can give rise to a detectable resonance event. Both assumptions find

their justification in experiment.

It should be remarked in this connection that the spacing value can be determined using the (γ,γ') technique only for nuclei where both Γ_γ and Γ_0/Γ_γ are relatively large, because only in this case is a large resonantly scattered signal observed. This condition is expected to be fulfilled for nuclei in the region of closed shells where the level density at low excitation is small. It is also expected that all resonance levels having a small Γ_0/Γ_γ, and hence a small Γ_0, will be missed in the present technique. This occurs because weak scattered signals will be generally masked by background and therefore will not show up in the scattered spectrum.

C. $E1$ and $M1$ Transitions

Among the ten resonances investigated in the present work, four were found to decay to the ground state by $E1$ transitions and two by $M1$ transitions. The other resonances were either weak (^{50}Cr and ^{109}Ag), and therefore it was impractical to measure their parity, or have isotropic angular distributions, and hence their scattered radiation is unpolarized (^{75}As and ^{205}Tl). Probably some of the most interesting results of the present work are the strong $M1$ transitions found in ^{141}Pr and ^{208}Pb. The level width of the $M1$ resonance in ^{141}Pr was found to be larger than the $E1$ resonance in the neighboring ^{139}La nucleus. The $M1$ radiation strength[30] is given by $K_{M1}=\Gamma_i(DE_i^3)^{-1}$, where D is the spacing of levels of the same spin and parity near the resonance energy. In order to get a rough estimate of the radiation strength, one may choose $D=700$ eV, which is probably an upper limit for the spacing of neutron resonances[22,23] of the same spin and parity at an excitation energy of about 7.6 MeV in ^{141}Pr. The radiation strength K_{M1} for the ground-state transition $7.632\rightarrow 0$ in ^{141}Pr is thus found to be 104×10^{-9} MeV^{-3}, to be compared with $K_{M1}=20\times10^{-9}$MeV^{-3} obtained by Bollinger,[31] who averaged the results of 17 $M1$ transitions from neutron resonances. The value of D selected above is higher than the value expected for the spacing of neutron resonances in this region of nuclei at such an excitation energy. Therefore, the $M1$ radiation strength in ^{141}Pr is at least five times higher than the average value.

The level width of the $M1$ resonance in ^{208}Pb seems to be higher than the average. The value of K_{M1} may be calculated by making a rough estimate of the spacing of 1^+ levels at 7.28-MeV excitation using the results of Biggerstaff *et al.*[32] regarding the ^{207}Pb (n,γ) reaction. These authors report a level spacing of 15 keV for 2^+ levels at an excitation energy of 7.4 MeV in ^{208}Pb. By introducing the appropriate spin factor, the level spacing for 1^+ levels may be found to be $D=25$ keV. The corresponding value of the radiation strength is $K_{M1}=81\times10^{-9}$ MeV^{-3}, which is a factor of 4 higher than the average value of the $M1$ radiation strength. It should be noted, however, that $M1$ transitions of similar strength were observed[32] in neighboring nuclei, namely, in ^{207}Pb using the ^{206}Pb(n,γ) reaction.

The $E1$ radiation strength[30] given by $K_{E1}=\Gamma_i\times(E_i^3DA^{2/3})^{-1}$ corresponding to the ground-state transitions of the four $E1$ resonances of Table III is also found to be generally higher than that of neutron resonances. This probably reflects the fact that the present technique selects those levels whose Γ_0 is relatively large.

More work remains to be done regarding the total widths of bound levels in order to find out whether the details of the systematic behavior of total radiative widths in neutron resonances persist for the case of bound levels.

ACKNOWLEDGMENTS

The authors wish to thank O. Shahal for help in the experimental measurements; thanks are also due to Y. Schlesinger for help in computer programming. One of us (R. M.) would like to acknowledge a helpful discussion with J. W. Knowles and A. M. Khan from Chalk River regarding polarization measurements.

[1]H. H. Fleischmann, Ann. Physik 12, 133 (1963).
[2]C. S. Young and D. I. Donahue, Phys. Rev. 132, 1724 (1963).
[3]G. Ben-David, B. Arad, J. Balderman, and Y. Schlesinger, Phys. Rev. 146, 852 (1966).
[4]B. Arad, G. Ben-David, I. Pelah, and Y. Schlesinger, Phys. Rev. 133, B684 (1964).
[5]S. Ramehandran and J. A. McIntyre, Phys. Rev. 179, 1153 (1969).
[6]M. Giannini, P. Oliva, D. Prosperi, and S. Sciuti, Nucl. Phys. 65, 344 (1965).
[7]B. Arad, G. Ben-David, and Y. Schlesinger, Phys. Rev. 136, B370 (1964).
[8]R. Moreh, O. Shahal, and S. Shlomo, Bull. Am. Phys. Soc. 13, 1368 (1968).
[9]K. Min, Phys. Rev. 152, 1062 (1966); G. P. Estes and K. Min, Phys. Rev. 154, 1104 (1967).
[10]R. Moreh and A. Wolf, Phys. Rev. 182, 1236 (1969).
[11]R. Moreh and O. Shahal, Phys. Rev. 188, 1765 (1969).
[12]W. E. Lamb, Phys. Rev. 55, 190 (1939).
[13]F. R. Metzger, Progr. Nucl. Phys. 7, 53 (1959).
[14]R. Moreh and A. Nof, Phys. Rev. 178, 1961 (1969).

[15]R. Moreh, D. Salzmann, and Y. Wand, Phys. Letters 30B, 536 (1969).
[16]M. Ferentz and N. Rosenzweig, in *Alpha-, Beta-, and Gamma-Ray Spectroscopy*, edited by K. Siegbahn (North-Holland Publishing Company, Amsterdam, The Netherlands, 1966), p. 1687.
[17]L. C. Biedenharn and M. E. Rose, Rev. Mod. Phys. 25, 729 (1953).
[18]L. W. Fagg and S. S. Hanna, Rev. Mod. Phys. 31, 711 (1959).
[19]F. Metzger and M. Deutsch, Phys. Rev. 78, 551 (1950).
[20]R. Moreh and M. Friedman, Phys. Letters 26B, 579 (1968). This article contains an error. The role of $E1$ and $M1$ transitions was reversed; thus the transitions from the resonance level in ^{62}Ni and ^{112}Cd are $E1$, while those in ^{141}Pr and ^{208}Pb are $M1$.
[21]G. A. Bartholomew, M. R. Gunye, and E. D. Earle, Can. J. Phys. 45, 2063 (1967).
[22]L. M. Bollinger, in *Nuclear Spectroscopy*, edited by F. Ajzenberg-Selove (Academic Press Inc., New York, 1960), Part A, p. 417.
[23]J. Julien *et al.*, Nucl. Phys. A132, 129 (1969).
[24]C. E. Porter and R. G. Thomas, Phys. Rev. 104, 483 (1956).
[25]K. Reibel and A. K. Mann, Phys. Rev. 118, 701 (1960).
[26]P. Axel, Phys. Rev. 126, 671 (1962).
[27]E. G. Fuller and E. Hayward, in *Nuclear Reactions*, edited by P. M. Endt and P. B. Smith (North-Holland Publishing Company, Amsterdam, The Netherlands, 1962), Vol. II, pp. 189–190.
[28]R. Moreh and A. Wolf, to be published.
[29]J. A. Harvey and G. G. Slaughter, Oak Ridge National Laboratory Report No. ORNL 3924, 1966 (unpublished), p. 28.
[30]G. A. Bartholomew, Ann. Rev. Nucl. Sci. 11, 259 (1961).
[31]L. M. Bollinger, in *International Symposium on Nuclear Structure, Dubna, 1968* (International Atomic Energy Agency, Vienna, Austria, 1969), p. 317.
[32]J. A. Biggerstaff, J. R. Bird, J. H. Gibbons, and W. M. Good, Phys. Rev. 154, 1136 (1967).

PHYSICAL REVIEW C VOLUME 2, NUMBER 3 SEPTEMBER 1970

Neutron Emission in Alpha-Particle-Accompanied Fission

Eran Nardi
Israel Atomic Energy Commission Soreq Research Center, Yavne, Israel and Weizmann Institute of Science, Rehovot, Israel

and

Zeev Fraenkel
Weizmann Institute of Science, Rehovot, Israel

(Received 6 April 1970)

A four-parameter correlation experiment which measured neutron emission in "long-range alpha" (LRA) fission is described. The energies of both the fission fragments and of the α particle as well as the time of flight of the neutron were recorded. The experimental data were analyzed with the aid of a computer, and the method of analysis is described.

Some of the results of the present experiment have already been published. In this paper we discuss the pre-neutron-emission mass distribution of LRA fission as well as some properties of the neutrons as a function of α-particle energy. In addition, the neutron kinetic energy as a function of fragment mass is given. The probability of α-particle emission as a function of the fission-fragment mass ratio is also discussed.

I. INTRODUCTION

At present there are two principal methods for studying the scission configuration of a fissioning nucleus. The first method is to investigate the properties of the prompt neutrons emitted from individual fission fragments, thereby obtaining information on the deformation energies of the various fission fragments at scission. These studies were summarized by Terrell.[1] The most important characteristic of the prompt neutrons in low-energy fission is the "saw tooth" dependence of the average number of neutrons as a function of fragment mass. The second method of obtaining information on the point of scission is by studying the properties of the α particles and fission fragments in "long-range alpha" fission (LRA fission). This process, which occurs about once in every 300 fission events, is characterized by the emission of an α particle in addition to the fission fragments. As has been discussed by Halpern[2] and by Fraenkel,[3] the fact that the α particle seems to be emitted at or very near the time of scission makes this particle extremely useful in studying the initial conditions at scission. The main conclusion obtained in studying the LRA fission process is